

THE NUMERICAL COMPUTATION OF INVARIANT CIRCLES OF MAPS

BY

I.G. KEVREKIDIS,

R. ARIS,

L.D. SCHMIDT,

AND

S. PELIKAN

IMA Preprint Series # 85

July 1984

**INSTITUTE FOR MATHEMATICS AND ITS APPLICATIONS**

**UNIVERSITY OF MINNESOTA**

**514 Vincent Hall**

**206 Church Street S.E.**

**Minneapolis, Minnesota 55455**

# THE NUMERICAL COMPUTATION OF INVARIANT CIRCLES OF MAPS

I.G. Kevrekidis<sup>1</sup>, R. Aris<sup>1</sup>, L.D. Schmidt<sup>1</sup>, and S. Pelikan<sup>2</sup>

<sup>1</sup> Department of Chemical Engineering and Materials Science  
and

<sup>2</sup> Institute for Mathematics and its Applications  
University of Minnesota  
Minneapolis, Minnesota 55455

## ABSTRACT

A method for the numerical computation of invariant circles of maps is presented, along with appropriate techniques for its implementation. The method involves solution of a functional equation by discretization and Newton iteration. The resulting algorithm is applied to a map of the cylinder and some examples of bifurcations of invariant circles are illustrated. Generalization of the method to the computation of invariant circles in more than two dimensions as well as sections of invariant tori is discussed.

(#) This work is partially supported by NSF under grant no. CPE 8313497

## INTRODUCTION

Invariant circles (closed curves) of maps arise in several contexts. They may appear when a fixed point of a map undergoes Hopf bifurcation [e.g.1]. If a system of ordinary differential equations has a periodic orbit, this orbit represents an invariant curve for the time  $t$  map. The curve may be filled with periodic points for the map, depending on the relationship between  $t$  and the period of the orbit. Transverse sections of invariant tori appear as invariant circles of the appropriate Poincare map (the stroboscopic map in the case of O.D.E.s with periodic forcing).

Perturbation techniques can be used to calculate such invariant circles [2] or invariant tori [3] close to Hopf bifurcation points in parameter space. It would be useful however, to numerically follow these invariant curves far from the initial bifurcation points, to obtain stability characteristics and to study their further bifurcations. Such numerical continuation involves the solution of a functional equation demanding that a closed curve in phase space be invariant under the appropriate transformation.

The purpose of this paper is to describe one method to accomplish this. The functional equation is "transformed" by discretization into a large system of nonlinear equations which is subsequently solved by Newton iteration. Both stable and unstable invariant circles of both invertible and noninvertible maps can be calculated. Stability information about these circles is contained - upon convergence - in the Jacobian of the Newton iteration. Information about the occurrence of resonances is contained in the structure of this Jacobian.

## THE PROCEDURE

We illustrate the procedure by discussing the special case of a map of the cylinder  $S^1 \times R$  given by  $F(\theta, x) = (g(\theta, x), f(\theta, x))$  where  $\theta \in S^1$  and  $x \in R$ . If a function  $x = r(\theta)$  has a graph which is mapped to itself by  $F$  then the graph represents an invariant curve. In this context we seek a solution of the equation

$$r(g(\theta, r(\theta))) = f(\theta, r(\theta)) . \quad (2)$$

Consider a discretization  $\{(\theta_i, r(\theta_i))\}$  .  $i = 1, 2, \dots, N$  of the graph of  $r(\theta)$ . Denote the images of these points under  $F$  by  $(\tilde{\theta}_i, \tilde{r}_i) = F(\theta_i, r(\theta_i))$ . These points constitute a discretization of  $\tilde{r}(\theta)$ , the image of the graph of  $r(\theta)$ . We wish to minimize the distance between the functions represented by these discretizations. Some kind of interpolation is necessary.

We might consider the functions to be close if  $r(\theta_i)$  is near  $r(\theta_j)$  for each  $i = 1, \dots, N$ . In this case, since in general the  $\tilde{\theta}_i$  do not coincide with any of the  $\theta_j$  we obtain an estimate  $\rho_i$  of  $\tilde{r}(\theta_i)$  by interpolation (e.g. through splines or finite element basis functions). We then solve (2) in the form

$$r_i - \rho_i = 0 \quad i = 1, 2, \dots, N \quad (3)$$

It can be seen that through this collocation scheme we consider that a curve and its image coincide - to within discretization and interpolation error - if their approximations coincide to within the truncation error of the computer at a number of discrete points. (see fig. 1)

An alternative procedure would be to ask that the integral

$$\int_0^{2\pi} (r(\theta) - \tilde{r}(\theta))^2 d\theta$$

be zero. Since this integral has to be estimated numerically, it will be a function of the  $r_i$  and  $\tilde{r}_i$  at the various values of  $\theta$  between 0 and  $2\pi$  that will be used in a Simpson or Gaussian quadrature estimation of (3).

In a Galerkin finite element approach, we approximate our function as  $r(\theta) = \sum \alpha_i \xi_i(\theta)$  where the  $\xi_i$  are a set of typical finite element nearly orthogonal basis functions. We then weigh the residual in (2) with these basis functions and demand that

$$\int_0^{2\pi} \xi_i(\theta) [r(\theta) - \tilde{r}(\theta)] d\theta = 0 \quad (5)$$

The above set of equations is then solved for the constants  $\alpha_i$  which occur in the expressions for  $r$  and  $\tilde{r}$ .

These procedures are justified if the points  $(\tilde{\theta}_i, \tilde{r}_i)$  actually represent a function: it is necessary that the points  $\tilde{\theta}_i$  remain in circular order. If this is not the case, a different parameterization of the invariant curve is required (e.g. percent total arclength, see below). For ease of discussion we now assume that parameterization with  $r$  as a function of  $\theta$  is appropriate, as is the case in the example as we are going to present.

All three techniques (3), (4), and (5) yield a set of nonlinear equations. All three demand that some estimate of the distance between  $r$  and  $\tilde{r}$  be small. In the present work we have used a collocation discretization, a cubic Lagrangian [4] interpolation, and Newton iteration for solving the system of nonlinear equations.

## STABILITY AND RESONANCES

It is interesting to consider the Jacobian of the Newton iteration upon convergence (which should be quadratic to the truncation error). From equations (2) and (3) we see that it will be of the form

$$\underline{\underline{J}} = \underline{\underline{I}} - [\partial\rho_i/\partial r_j] \quad (6)$$

where  $\underline{\underline{I}}$  is the unit matrix. Since, according to our construction, each  $\rho_i$  depends only on those  $r_j$  that were used in the interpolation - for example the nearest four for cubic interpolation - the Jacobian will be a sparse matrix, with 1 along the diagonal, and a band (a generally nonstraight, four element wide strip) traversing it from top to bottom. Given the periodicity of the problem, if the band crosses the right edge of the matrix it reappears on the left (see fig. 2).

As the number of discretization points goes to infinity, the "slope" of this band can be estimated, and it will indicate whether the map is locally contracting or expanding.

There are two important points to be observed about this matrix. The first is that it contains stability information for the calculated invariant curve. Let  $\lambda_i$  be the eigenvalues of  $\underline{\underline{J}}$  and  $\psi_i = 1 - \lambda_i$  the eigenvalues of  $[\partial\rho_i/\partial r_j]$ . The invariant circle changes stability as one or more of the  $\psi_i$  cross the unit circle. In the case of loss of stability of an invariant curve to a period 2 invariant curve a  $\psi_i$  goes through -1 (and some  $\lambda_i$  through 2). If the second iterate of the map is used for the computation of the invariant curve, then  $\psi_i^2$  goes through 1 and the Jacobian changes sign (becoming singular as some  $\lambda_i$  goes through 0). Singularity of the Jacobian is also observed in turning point bifurcations. Pseudo-arc-length continuations and branch switching at bifurcation points can be used in a systematic bifurcation analysis to overcome this singularity and to follow bifurcating branches in parameter space. [5,6]

The most important characteristic of the Jacobian however, is that resonances (periodic points on the invariant curve, phase locking on the torus) appear as crossings of the four-element wide band and the diagonal for the Jacobian corresponding to the appropriate iterate of the map (see fig. 3). Such crossings provide good initial guesses for algorithms designed to compute periodic points. It can then be seen that the problem decomposes into smaller "local" problems of constructing saddle-node connections.

The elements of the Jacobian may not have exactly the same values for different discretizations and iterative techniques; the structure of the Jacobian however, is characteristic of the problem, and should be the same for all methods. Sparse matrix techniques can be used for efficient inversion of such a matrix [7].

## AN EXAMPLE

In order to illustrate the method we studied some aspects of the parameter dependence of the invariant curves of a specific map of the cylinder. This map is given by

$$\begin{aligned}\theta_{n+1} &= \theta_n + \omega \\ x_{n+1} &= \lambda x_n(1 - x_n) + \varepsilon \cos \theta_n\end{aligned}\tag{7}$$

where  $\lambda$ ,  $\varepsilon$  and  $\omega$  are parameters.

When  $\varepsilon = 0$  the coordinates are uncoupled and the  $x$  coordinate is transformed according to the logistic map. Invariant curves occur and bifurcate at the same values of  $\lambda$  for which periodic points occur and bifurcate in the logistic map. When  $\varepsilon > 0$  this is no longer the case. For example, the attracting period 2 curve which corresponds to the attracting period 2 orbit of the logistic map does not undergo a period doubling bifurcation with increasing  $\lambda$  if  $\varepsilon$  is bigger than some critical value. Instead, the curve becomes increasingly irregular and finally disappears. It is replaced by a "strange looking" attractor. A similar bifurcation may be observed when  $\lambda$  is fixed and  $\varepsilon$  is increased. For a discussion of the mechanism which prevents the curve from period doubling, see [8]. This type of bifurcation - an interrupted period doubling cascade - has been observed in other contexts [9] and appears to represent another "route to chaos".

In a series of figures (4,5,6,7) we present some aspects of the bifurcations of this map, computed with our algorithm. We have included some comparisons with results of numerical simulation as well.



## DISCUSSION

This paper presents an algorithm which we believe will prove valuable in the study of certain aspects of the bifurcation behavior of maps and of dynamical systems in general. The purpose is to demonstrate that, with such an algorithm, one can obtain information that would require many thousands of point iterates, or that might not be practical to obtain through simulations at all. This information includes stability characteristics which assist and complement bifurcation analyses.

Some important characteristics of the scheme are that it is applicable in situations where the invariant curves are unstable, where the map is not invertible, and also in cases of resonance.

The example we considered was simple because it had an obvious parameterization. The generalization of the method to maps from  $\mathbb{R}^n$  to  $\mathbb{R}^n$  is straightforward once an appropriate parametrization has been found. For example, a simple polar coordinate representation would not be appropriate for an invariant circle of some map of the plane which intersects radial lines more than once. In such cases we have used a percent arclength parameterization which, however, lacks the computationally appealing characteristic of producing a sparse Jacobian. Since the total arclength depends on all points of the discretized curve, the Jacobian becomes a full matrix. Arclength parametrizations permit a generalization of the method to maps in higher dimensions. We feel that the computational savings provided by sparse matrix techniques, however, would probably justify the search for some ad hoc parameterization appropriate for a particular problem in a particular region of its parameter space.

To find invariant tori of systems of O.D.E.s, one may compute invariant curves of the Poincare map associated with some transverse section of the torus. In such cases, since the iterate of a point will be calculated by integrating

the system equations, the derivatives of the map will be estimated by simultaneous integration of the variational equations. An alternative approach would be to discretize and solve for the entire invariant surface. This would have the advantage that it would not require lengthy numerical integrations. Two parameters would be necessary to describe the invariant surface and the resulting system of equations would be very much larger for such a method.

We are aware of two other algorithms in the literature with the same objective. The first [10] computes one point on the invariant circle, the second [11] solves for the invariant circle along with its rotation number. We feel that these algorithms may run into difficulties in cases where periodic points exist on the invariant curve. The second algorithm has so far been implemented in [11] using a Fourier expansion of the invariant curve, and is currently being implemented by E. Doedel using piecewise polynomial representation. Such an algorithm would produce sparse Jacobians, similar in nature to the ones we have described.

We feel that numerical investigation of the type of bifurcation illustrated in Fig. 5, in which the invariant curve becomes increasingly irregular is a challenging task since an increasingly finer discretization is required to resolve these irregularities. If, as we suspect, the curve is non-rectifiable at the point of bifurcation, it could not be computed and some extrapolation would be required to determine the bifurcation point.

Currently we are applying the algorithm to the following problems: the delayed logistic map studied by Aronson et. al. [12]; the tori resulting from a system of periodically forced O.D.E.s [13]; and a detailed investigation of our example map (7).

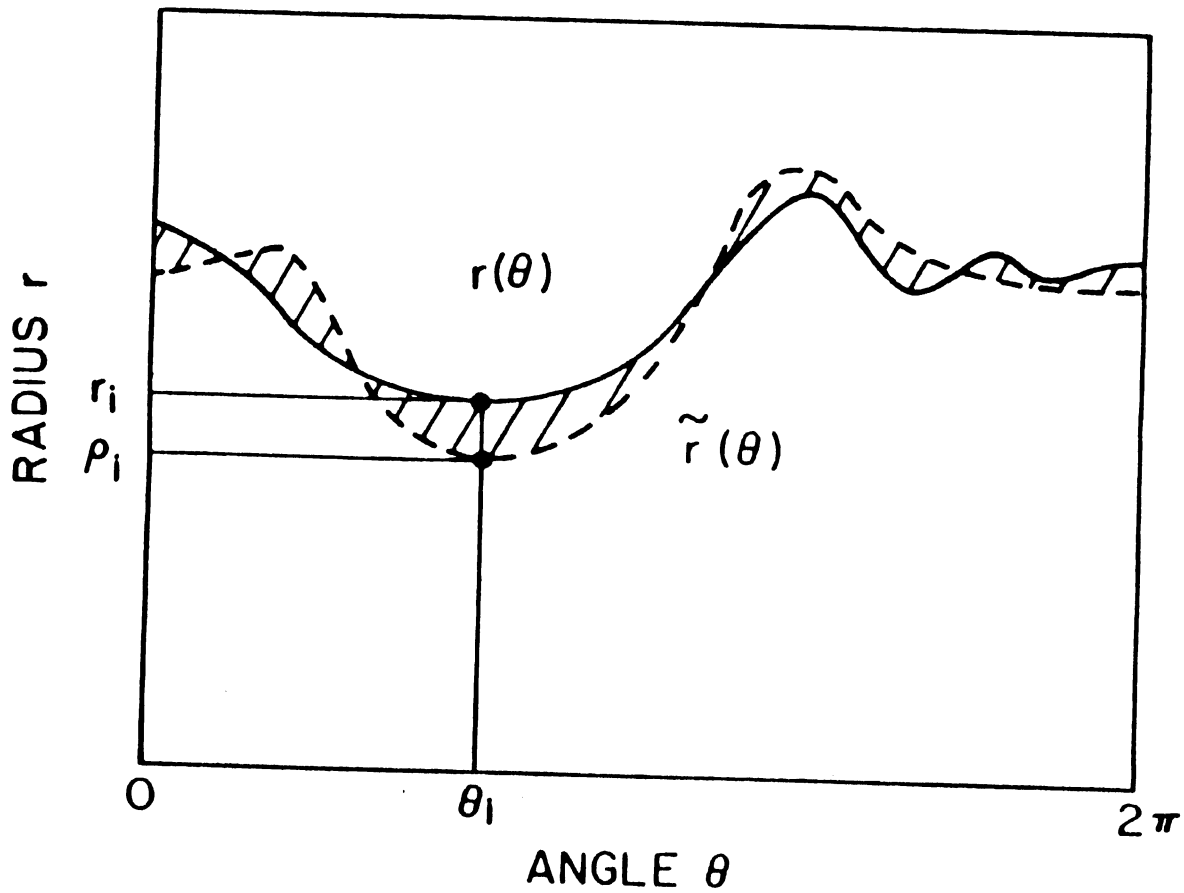


Fig. 1

Illustration of the collocation scheme for the computation of an invariant curve. We consider that the curve  $r(\theta)$  and its image  $r(\theta)$  coincide when the distances  $|r_i - \rho_i|$  at the discretization points  $\theta_i$  are zero.

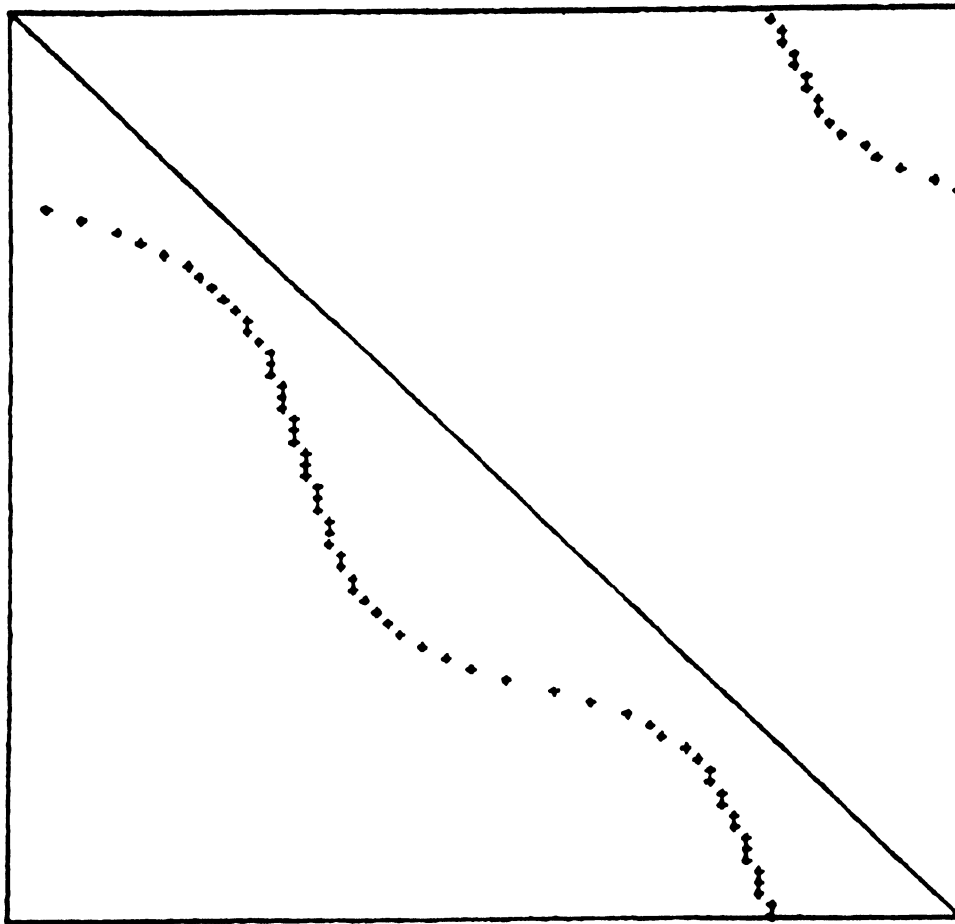


Fig. 2

Typical structure of the Jacobian  $\underline{J}$  after convergence. Dots indicate the approximate location of the band of off-diagonal non-zero entries.

This particular matrix arose in the computation of the invariant curve of the Poincare map of the forced Brusselator [13]

$$\begin{aligned} \dot{x} &= x^2 y - bx + a - x + d \cos \omega t \\ \dot{y} &= bx - x^2 y \end{aligned}$$

for  $a = 0.4$ ,  $b = 1.2$ ,  $\omega = 0.445$ ,  $d = 0.0072$ . A polar coordinate parametrization was used with centerpoint  $x = .372$   $y = 3.12$ , eighty equally spaced discretization points, and two-point linear interpolation.

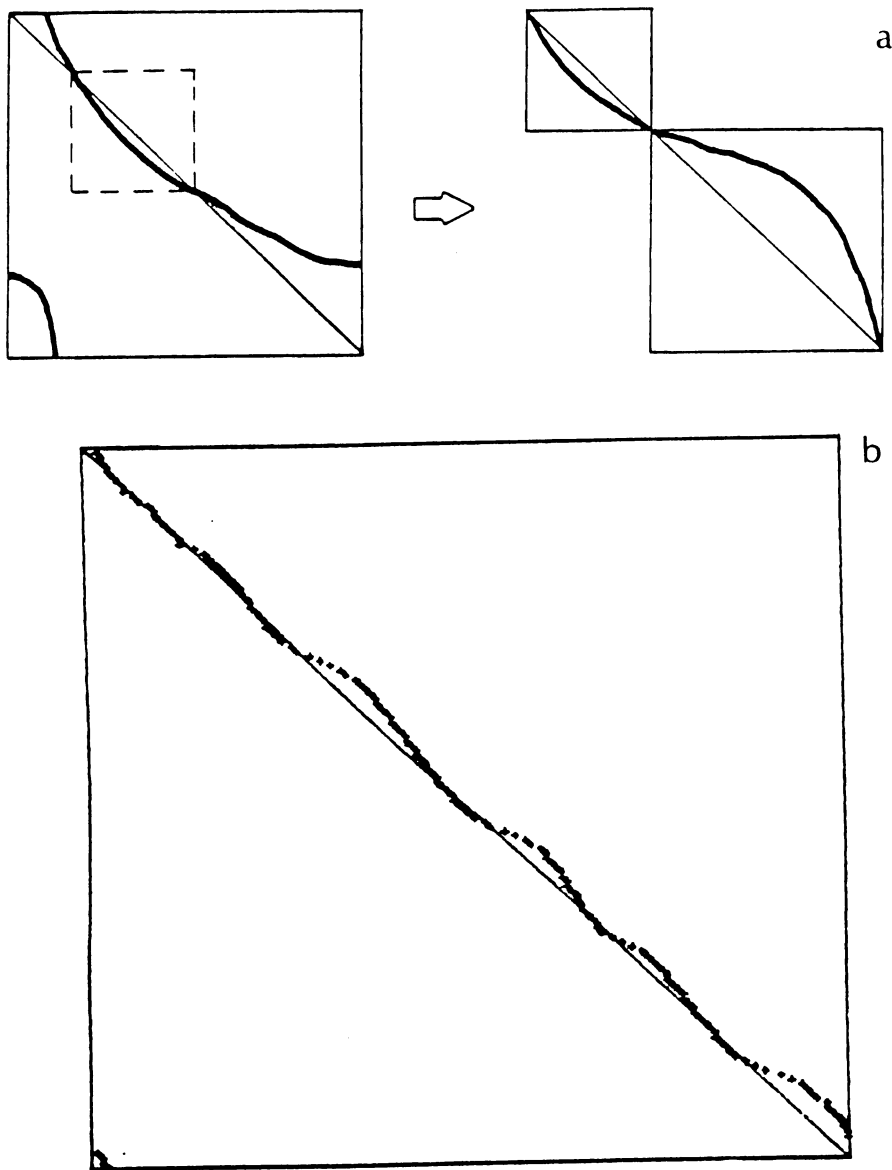


Fig. 3

(a) Typical structure of a Jacobian with resonances. (left) Notice how the problem decomposes into smaller uncoupled problems.

(b) Structure of the Jacobian of the calculation of an invariant circle through the seventh iterate of the delayed logistic map [12]

$$\begin{aligned}x_{n+1} &= y_n \\ y_{n+1} &= ay_n(1 - x_n)\end{aligned}$$

for  $a = 2.1771$ . Crossings of the diagonal indicate periodic points. Polar coordinate representation with centerpoint at  $x = y = \frac{a-1}{a}$ , 150 evenly spaced discretization points with two-point linear interpolation.

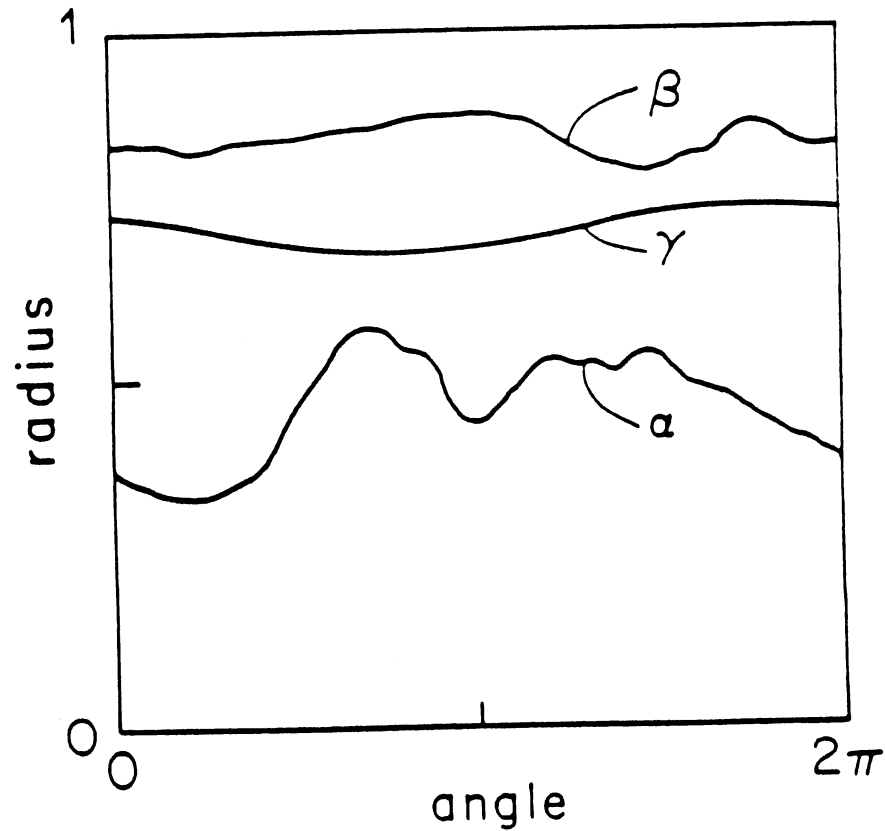


Fig. 4

Invariant curves of the map (7) for  $\lambda = 3.46$ ,  $\epsilon = 0.032$ ,  $\frac{\omega}{2\pi} = \frac{\sqrt{5} - 1}{2}$ . The results obtained by our method and through simulation are superimposed. The corresponding curves differ by less than  $10^{-4}$ . Curves ( $\alpha$ ) and ( $\beta$ ) are invariant for the second iterate of the map. Curve ( $\gamma$ ) is invariant for every iterate. Numerical computation was done using 160 evenly spaced discretization points and cubic interpolation. Curves ( $\alpha$ ) and ( $\beta$ ) are attractors and were drawn by a simulation in which 100,000 iterates of a point were plotted (after 4000 preiterations). Curve ( $\gamma$ ), which is unstable, was obtained by iterating one of the two branches of the inverse mapping.

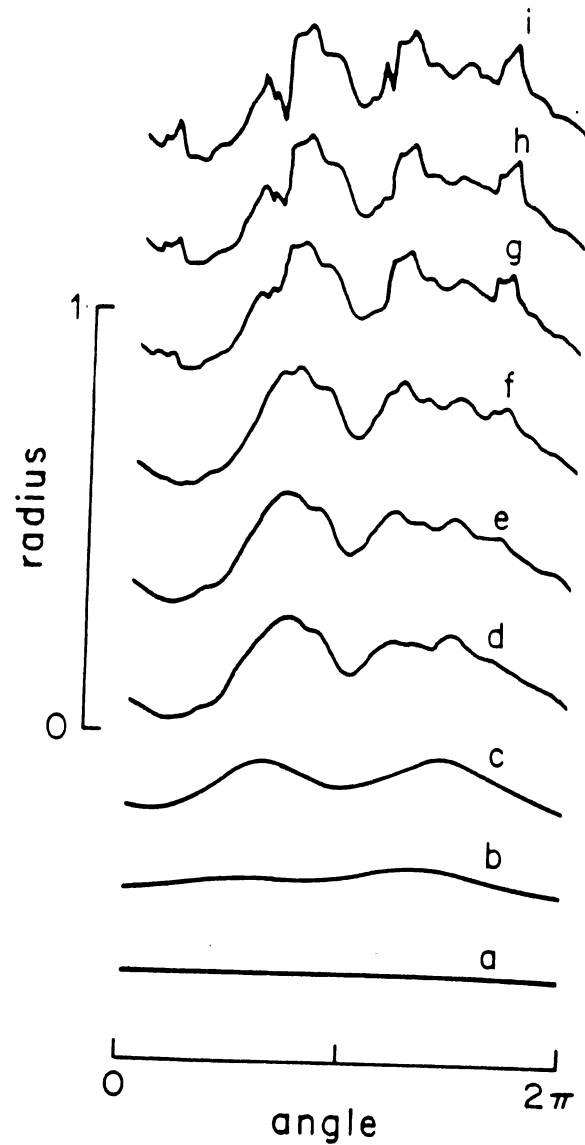


Fig. 5

Evolution of one of period two curves (the lower one,  $(\alpha)$  in Fig. 4) with varying  $\epsilon$  for  $\lambda = 3.46$  and  $\omega/2\pi = (\sqrt{5} - 1)/2$  drawn with our method as described in fig. 4.

a	$\epsilon = 0.001$	$r(0) = .43560$
b	$\epsilon = 0.01$	$r(0) = .41195$
c	$\epsilon = 0.02$	$r(0) = .38490$
d	$\epsilon = 0.032$	$r(0) = .37547$
e	$\epsilon = 0.033$	$r(0) = .37451$
f	$\epsilon = 0.034$	$r(0) = .37392$
g	$\epsilon = 0.0349$	$r(0) = .37501$
h	$\epsilon = 0.0351$	$r(0) = .37388$
i	$\epsilon = 0.0352$	$r(0) = .37291$

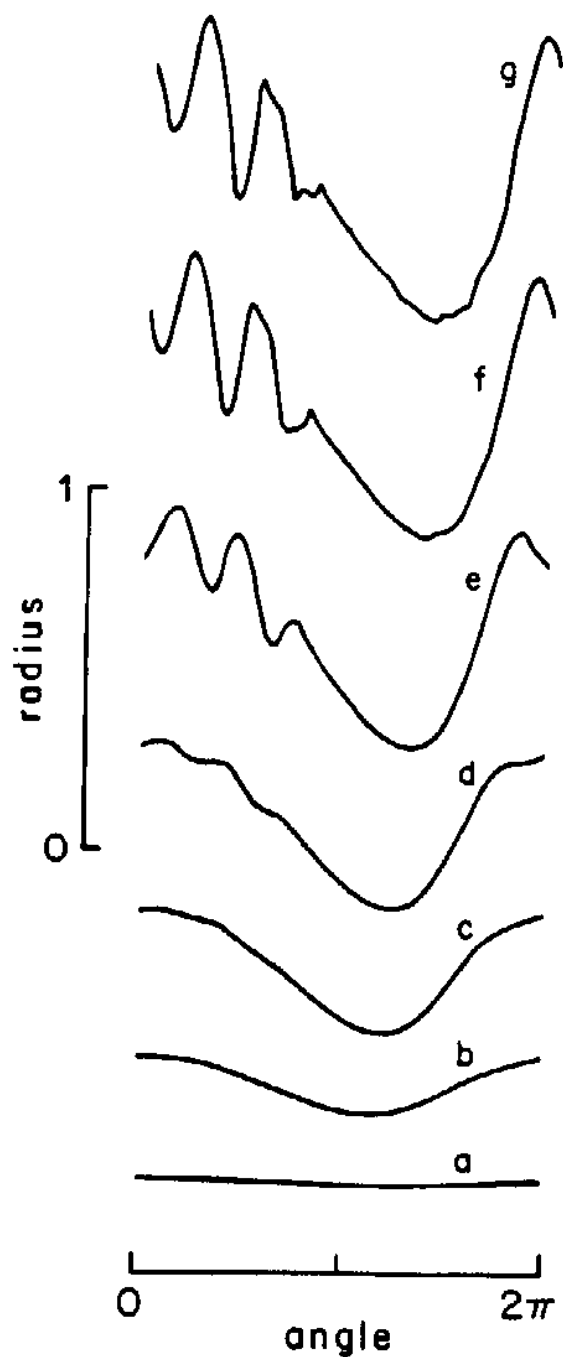


Fig. 6

Evolution of an invariant period one curve of the map (7) for  $\lambda = 2.5$ ,  $\omega = .5$  as  $\epsilon$  varies, drawn with our method as described in fig. 4.

a	$\epsilon = 0.01$	$r(0) = .60643$
b	$\epsilon = 0.1$	$r(0) = .66016$
c	$\epsilon = 0.2$	$r(0) = .71332$
d	$\epsilon = 0.25$	$r(0) = .73386$
e	$\epsilon = 0.3$	$r(0) = .69901$
f	$\epsilon = 0.325$	$r(0) = .74377$
g	$\epsilon = 0.33$	$r(0) = .80768$



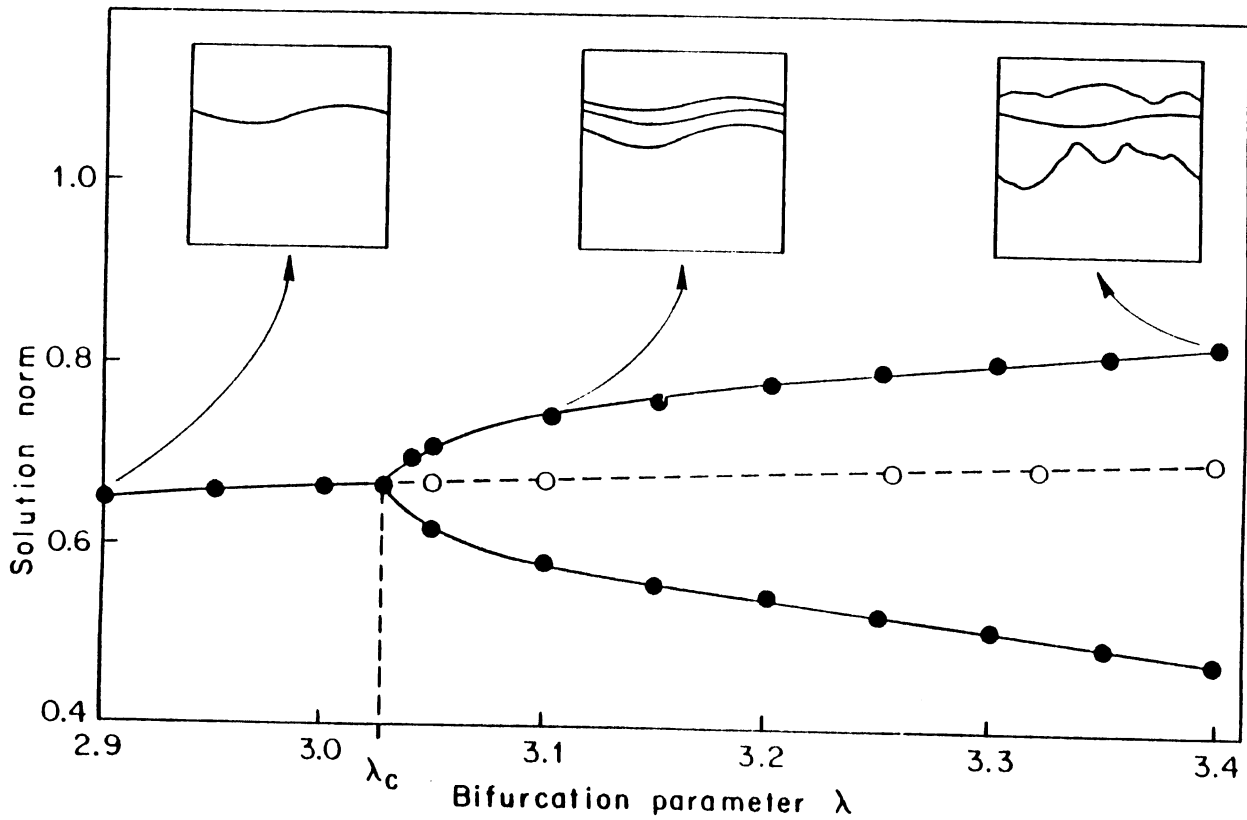
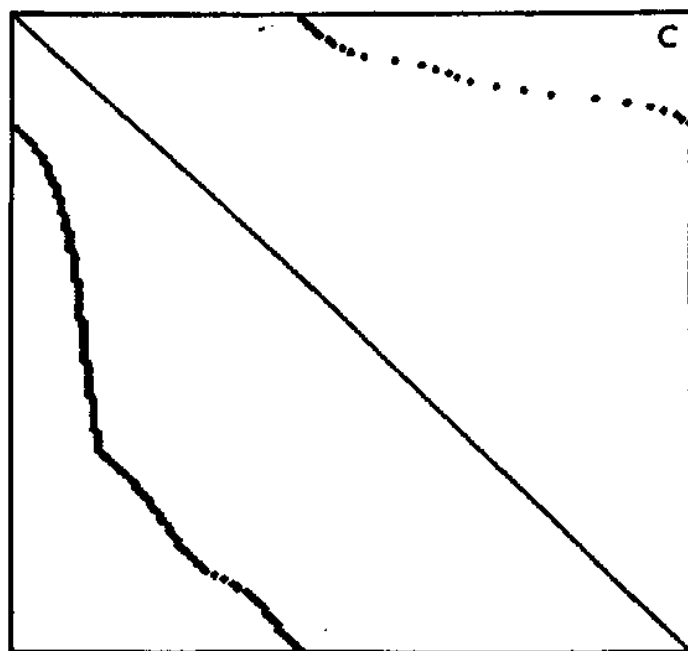
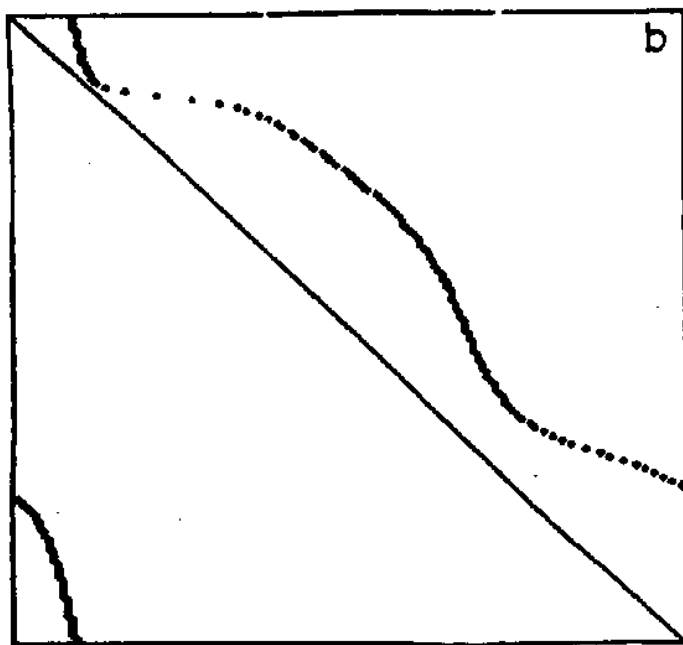
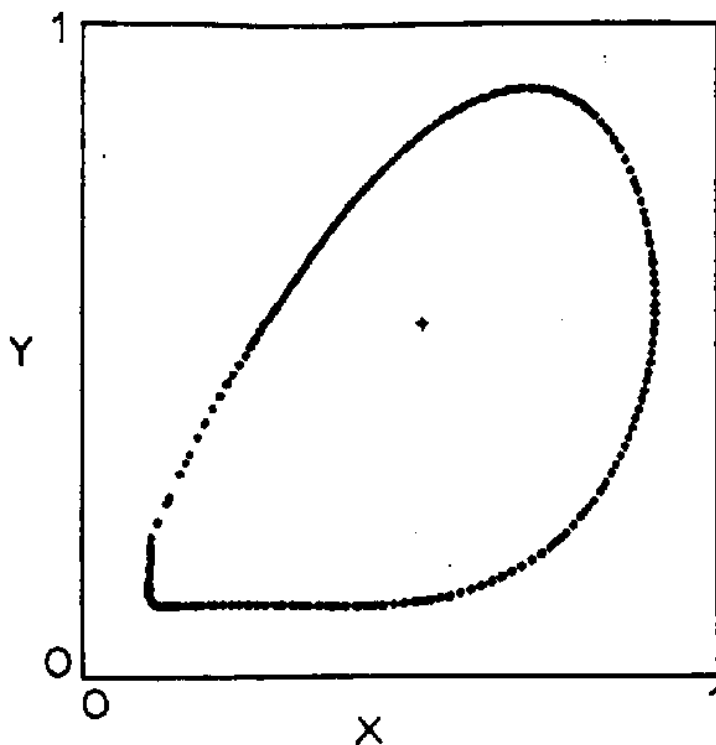


Fig. 7

Bifurcation diagram of the map (7) for  $\omega/2\pi = \frac{\sqrt{5}-1}{2}$ ,  $\varepsilon = 0.032$ . The quantity  $\sqrt{\sum(r_i^2)/N}$  where  $\{r_i\}$ ,  $i = 1, \dots, 160$  is a discretization of invariant curves obtained by our algorithm, is plotted vs. the bifurcation parameter  $\lambda$ . At  $\lambda = \lambda_c$  the invariant period one loses stability and two period-two curves bifurcate from it. The approximate shape of these invariant curves for various values of  $\lambda$  is shown by the insets.



**FIGURE 8.**

(a) Invariant circle of the delayed logistic map (see caption fig.3b) for  $a=2.1771$  when the rotation number is  $1/7$ . Polar parameterization (origin denoted by +) with 150 evenly spaced mesh points. The first iterates of the solution points are also plotted.

(b)&(c) Jacobian structure for the computation of the invariant circle in (a) through the first (b) and the fourth (c) iterate of the map. Crossings occur at the 7-th iterate Jacobian shown in fig.3b, since periodic points of period 7 exist on the invariant circle.

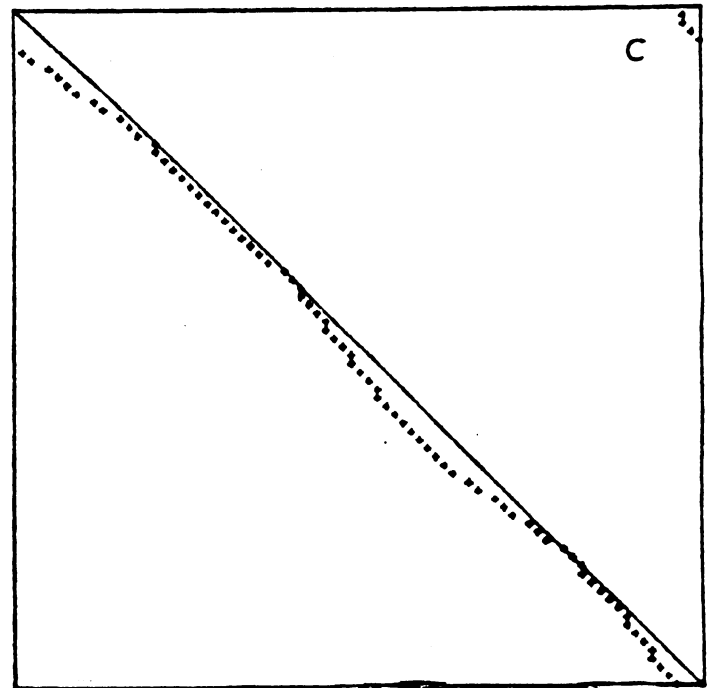
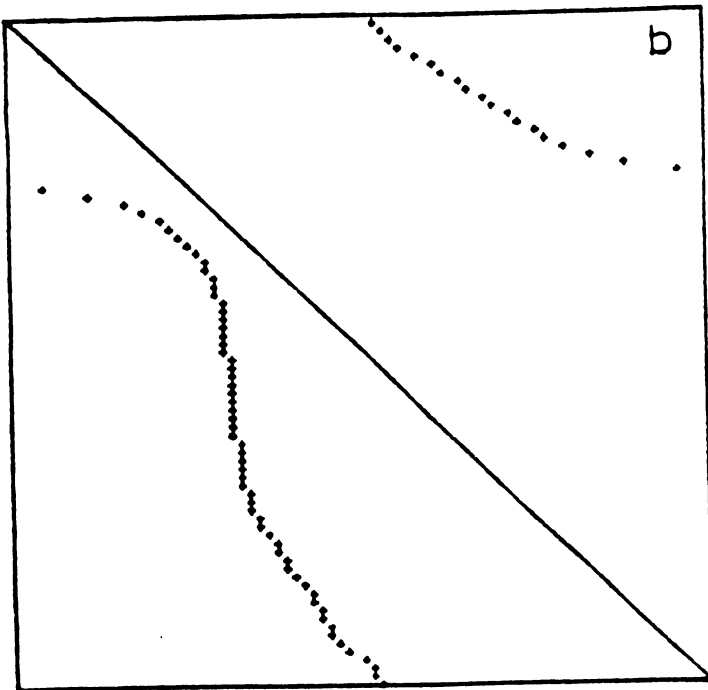
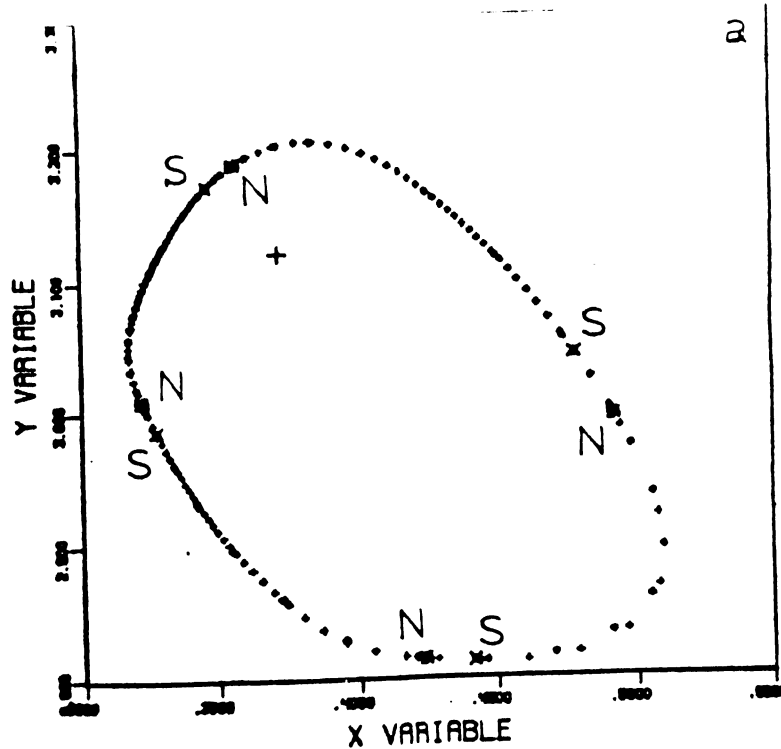


FIGURE 9.

Example of an invariant torus with subharmonics locked on it.

(a) Section of the invariant torus of the forced Brusselator (see caption fig.2) for  $d=0.0072$  and the ratio of the forcing to the natural frequency is  $4/3$ . Polar parameterization with 80 evenly spaced mesh points (origin denoted by +). The four nodes N and the four saddles S belong to the subharmonic periods 4 locked on the torus. They have been calculated through an entirely independent algorithm for the computation of fixed points of the stroboscopic map.

(b) & (c) Jacobian structure for the computation of the torus section in (a). through the first (b) and the fourth (c) iterate of the map. The crossing of the diagonal corresponding to the lowest S-N pair in (a) has been missed in (c) due to the coarseness of the even polar mesh at that region.

## ACKNOWLEDGEMENTS

We would like to thank Prof. R. McGehee and Prof. G. Sell for helpful discussions. Prof. E. Doedel was particularly generous in describing his current research. I.G.Kevrekidis acknowledges the support of the Graduate School of the University of Minnesota through a Stanwood-Johnston fellowship.

## REFERENCES

1. Marsden J.E. & McCracken M. The Hopf bifurcation and its applications. Appl.Math.Sci. 19, Springer Verlag 1976.
2. G. Iooss, A. Arneodo, P. Coullet, C. Tresser. Simple computation of bifurcating invariant circles for mappings. Lect. Notes in Math. 898 p. 192-211 Springer Verlag 1981 (& references therein).
3. Iooss G. & D.D. Joseph. Elementary Stability and Bifurcation Theory. U.T.M. Springer Verlag 1980.
4. Carnahan, B., Luther, H.A. & Wilkes, J.O. Applied numerical methods. John Wiley and Sons, 1969.
5. Keller, H.B. Numerical Solution of bifurcation and nonlinear eigenvalue problems. Applications of Bifurcation Theory, P.H. Rabinowitz ed. Academic Press, 1977, pp. 359-384.
6. E. Doedel. Continuation Techniques in the study of Chemical Reaction Schemes. to appear in Proc. Special Year in Energy Math. U. of Wyoming, K.I. Gross ed., SIAM Publ.
7. Eisenstat, S.C., Gursky, M.C., Schultz, M.H. & Sherman, A.H. Yale Sparse Matrix Package II. The nonsymmetric codes. Research report #114, Yale University, Department of Computer Science.
8. Grebogi, C., E. Ott, S. Pelikan, J. Yorke. Strange attractors that are not chaotic. To appear, Physica D.
9. Francheschini, V. Bifurcation of Tori and phase locking in a dissipative system of differential equations. Physica D(1983) #3, 285-304.

10. E. Thoulouze-Pratt. Numerical analysis of the behaviour of an almost periodic solution to a periodic differential equation, an example of successive bifurcation of invariant tori. in Lecture Notes in Biomathematics, 49 Springer Verlag 1983 pp. 265-271.
11. E. Doedel. private communication 1984  
and  
Chan, T.N. "Numerical Bifurcation Analysis of Simple Dynamical Systems" M. Comp. Sci. Thesis, Concordia University, September 1983.
12. Aronson, D.G., Chory, M.A., Hall, G.R. and McGeehee, R.P. Bifurcations from an Invariant Circle for Two-Parameter Families of Maps of the Plane: A Computer-Assisted Study. Commun. Math. Phys. 83, 303-354 (1982).
13. K. Tomita. Chaotic response of nonlinear oscillators. Physics reports 86, No. 3, pp. 113-167, 1982.